



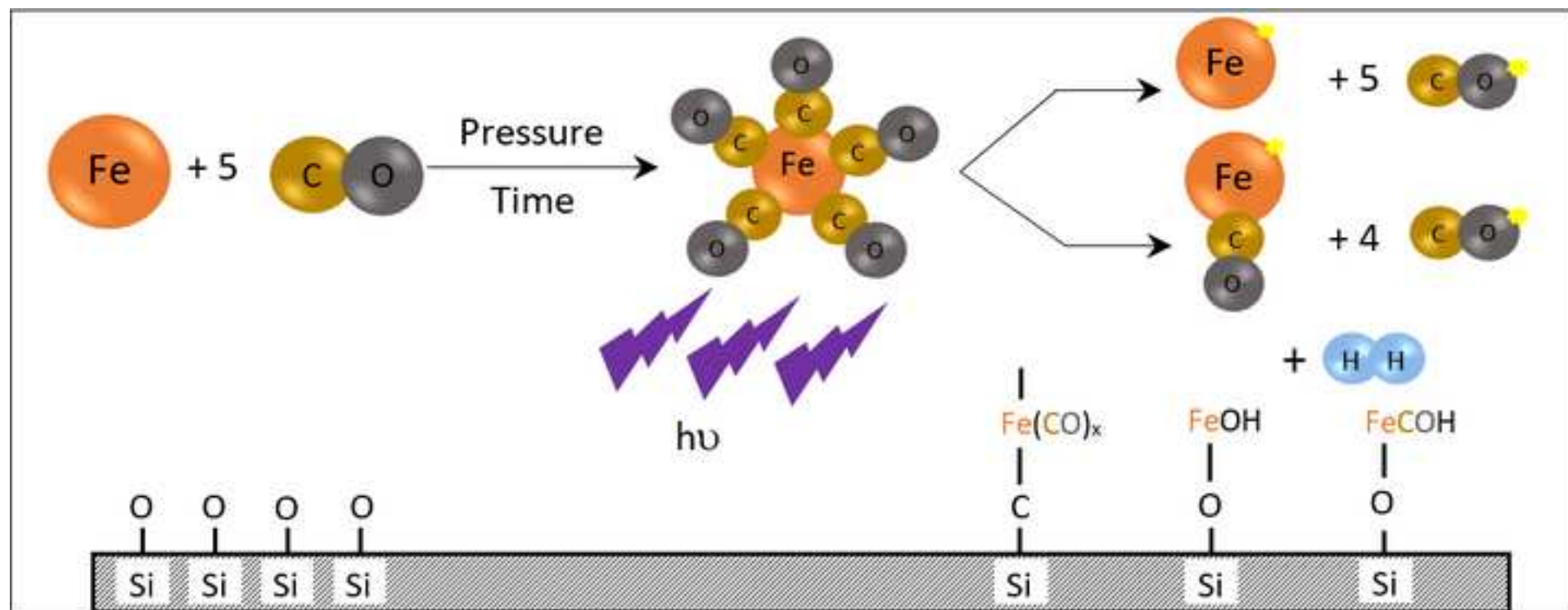
<b>Titre:</b> Title:	Shedding light on iron pentacarbonyl photochemistry through a CVD case study
<b>Auteurs:</b> Authors:	Hamed Nasri Lari, Donya Farhanian, Daria Camilla Boffito, Gregory Scott Patience, Gregory De Crescenzo, Jamal Chaouki, & Jason Robert Tavares
<b>Date:</b>	2017
<b>Type:</b>	Article de revue / Article
<b>Référence:</b> Citation:	Nasri Lari, H., Farhanian, D., Boffito, D. C., Patience, G. S., De Crescenzo, G., Chaouki, J., & Tavares, J. R. (2017). Shedding light on iron pentacarbonyl photochemistry through a CVD case study. <i>Catalysis Communications</i> , 100, 19-23. <a href="https://doi.org/10.1016/j.catcom.2017.06.024">https://doi.org/10.1016/j.catcom.2017.06.024</a>

 **Document en libre accès dans PolyPublie**  
Open Access document in PolyPublie

<b>URL de PolyPublie:</b> PolyPublie URL:	<a href="https://publications.polymtl.ca/2792/">https://publications.polymtl.ca/2792/</a>
<b>Version:</b>	Version finale avant publication / Accepted version Révisé par les pairs / Refereed
<b>Conditions d'utilisation:</b> Terms of Use:	CC BY-NC-ND

 **Document publié chez l'éditeur officiel**  
Document issued by the official publisher

<b>Titre de la revue:</b> Journal Title:	Catalysis Communications (vol. 100)
<b>Maison d'édition:</b> Publisher:	Elsevier
<b>URL officiel:</b> Official URL:	<a href="https://doi.org/10.1016/j.catcom.2017.06.024">https://doi.org/10.1016/j.catcom.2017.06.024</a>
<b>Mention légale:</b> Legal notice:	© 2017. This is the author's version of an article that appeared in <i>Catalysis Communications</i> (vol. 100) . The final published version is available at <a href="https://doi.org/10.1016/j.catcom.2017.06.024">https://doi.org/10.1016/j.catcom.2017.06.024</a> . This manuscript version is made available under the CC-BY-NC-ND 4.0 license <a href="https://creativecommons.org/licenses/by-nc-nd/4.0/">https://creativecommons.org/licenses/by-nc-nd/4.0/</a>



## \*Highlights (for review)

- Formation of iron pentacarbonyl in a pressurized CO cylinder changes the photoreaction path
- Photoreaction highly depends on the UV wavelength under atmospheric pressure
- Fe(CO) and Fe are substantial species which play the role of catalytic initiators

# Shedding Light on Iron Pentacarbonyl Photochemistry Through A CVD Case Study

Hamed Nasri Lari<sup>†</sup>, Donya Farhanian<sup>†</sup>, Daria C Boffito, Gregory S Patience, Gregory De Crescenzo, Jamal Chaouki, Jason R. Tavares<sup>1</sup>

Department of Chemical Engineering, École Polytechnique de Montréal, C.P. 6079, Succ. Centre-Ville, Montreal, Quebec Canada H3C 3A7

## Abstract

During our studies on surface engineering, we photopolymerize syngas onto silicon surfaces. XPS and TOF-SIMS analyses show that the syngas-derived oligomer covalently bonds to free silanol sites. Iron atoms appear in the coating, despite the fact that no iron was (intentionally) added to the system. GC-MS analysis reveals low concentrations of iron pentacarbonyl (IPC) are generated within the carbon monoxide cylinder. Its presence plays a determinant photocatalytic role in the reaction.

*Keywords: photochemistry, iron pentacarbonyl, syngas, photo-initiated chemical vapor deposition (PICVD), photopolymerization.*

## 1. Introduction

Iron pentacarbonyl (IPC –  $\text{Fe}(\text{CO})_5$ ) is a monomeric metal carbonyl that is sensitive to air, heat, and light. Iron reacts with carbon monoxide to form IPC at high pressure ( $> 20$  MPa) and temperature below  $200$  °C, and decomposes above  $230$  °C into Fe, CO and secondary carbonyls. When syngas, or carbon monoxide is stored at high pressure, iron can foul heat transfer surfaces and other process equipment when IPC decomposes [1, 2]. IPC, like most metal carbonyls, is volatile and, when exposed to sunlight, liquid IPC solidifies [3]. This property opened up a dedicated field of research devoted to organotransition metal complexes [4-6]. Metal carbonyls have been used as photocatalysts in various liquid [7, 8] and gas phase [9-12] UV reactions where light removes ligands to generate a coordinatively unsaturated catalyst. IPC-photocatalyzed reactions in the liquid phase have been extensively studied in i) isomerization, ii) hydrogenation of olefins, and iii) hydroformylation of alkenes [10-12].  $\text{Fe}(\text{CO})_3$  [13] or  $\text{Fe}(\text{CO})_4$  [8] are the active species. Isomerization and hydrogenation of olefins and alkenes have also been investigated in the gas phase in the presence of metal carbonyl compounds.  $\text{Cr}(\text{CO})_6$  and 1-butene isomerizes n-butane to 2-butene in the presence of 248-nm exciplex laser light. They react differently in the gas phase compared to the liquid phase due to higher photofragmentation degree [10]. Whetten et al. [11], through kinetic studies, showed that the gas phase catalytic pattern was analogous to that found in liquids. However, quantum yields are higher in the gas phase. Poliakoff and Weitz [8] also reported that more CO groups dissociate in the gas phase compared to the liquid phase: more than one CO groups dissociate from IPC by absorption of single UV photon, due to collisional relaxation efficiency [14]. Therefore, the higher the unsaturated intermediates, the greater the yield. Hence, through direct monitoring of intermediate transient species, all studies concluded that the coordinatively unsaturated catalysts are in the form of  $\text{Fe}(\text{CO})_4$  in the liquid phase, and  $\text{Fe}(\text{CO})_3/\text{Fe}(\text{CO})_2$  in the gas phase.

---

<sup>1</sup> Corresponding author. Tel: +1-514-340-4711 Ext. 2326; fax: +1-514-340-4159  
E-mail address: jason.tavares@polymtl.ca

<sup>†</sup> These authors contributed equally to the study.

1  
2  
3  
4 So far, the photocatalytic behavior of IPC has not been reported in the context of polymerization  
5 reactions. Moreover, very little research has reported the photocatalytic behavior of IPC under normal  
6 temperature and pressure (Fig. 1). Since the product distribution of metal carbonyl photolysis in the gas  
7 phase is wavelength- and pressure-dependent [15], studying reactions under atmospheric pressure and  
8 UVC radiation can provide a better understanding of IPC photoreactions.  
9

10  
11 During our studies on surface modification through photo-initiated chemical vapor deposition (PICVD)  
12 [16-19], we observed that the reaction of syngas and hydrogen peroxide under UVC radiation provided by  
13 low-pressure mercury (germicidal) lamps produced a yellowish film on the surface of silicon wafer  
14 substrates (110, type N) and the quartz reactor walls. Although operating conditions, molar ratio of  
15 reactants, and reaction time remained constant through a series of experiments, the color of silicon wafer  
16 would change to a darker brown-yellow color over time (Fig. 2c/top). XPS analyses revealed the presence  
17 of iron in the film (Supporting Information Fig. 1S, Table 1S), and FTIR spectroscopy identified the  
18 presence of functional groups in the deposited layer (Supporting Information Fig. 2S).  
19  
20

21 Here, we report evidence that small concentrations of IPC in the gas phase accelerate the polymerization  
22 of syngas through generating active intermediates in the gas phase. Further, the molecular structure of the  
23 film showed that oligomer chains were dominantly bonded to the silicon surface through Fe(CO)  
24 fragments.  
25  
26

27 Fig. 1 Operating conditions of previous photolytic reactions [20].  
28

## 29 **2. Experimental**

30 The experimental protocol for PICVD treatment is reported in detail in previous works [19]. Briefly, to  
31 prepare the substrates, silicon coupons were first cleaned by soaking in an ultrasonic bath of isopropanol  
32 for 10 minutes, then drying with compressed air. In each PICVD experiment, a quartz tube reactor (225  
33 cm<sup>3</sup> internal volume, standard 24/40 taper joints, Montreal Glassblowing Inc.) was first purged with argon  
34 for 5 minutes. H<sub>2</sub> and CO were introduced to the reactor at a constant molar ratio of one (total flow of 0.2  
35 L/min). The reaction was initiated using 28 UVC germicidal lamps (irradiance of 0.012 W cm<sup>-2</sup> at a  
36 distance of 33 cm). After two hours, the reaction was stopped by turning off the UVC lamps and  
37 switching the reactant flows to argon for a final purge.  
38

39 In order to identify the iron source, two high-pressure carbon monoxide cylinders (99.99% Air Liquide  
40 Canada) were analyzed using GC-MS (Agilent 5975C VL MSD Triple Axis, equipped with a 30 m / 0.25  
41 mm / 0.25 μm DB-wax column). One cylinder was recently purchased, whereas the other was six-months  
42 old. Hereafter, these are referred to as the new and old cylinders, respectively. We sampled each cylinder  
43 and injected 5 μL aliquots into the GC-MS. The injector and detector temperatures were 300 and 250 °C,  
44 respectively. In the analytical protocol, the GC-MS oven temperature was kept constant at 45 °C for  
45 20 min, followed by a ramp in 20 °C/min up to 230 °C, with 0.5 mL min<sup>-1</sup> He as the carrier gas. The GC-  
46 MS signal was calibrated with (under carbon dioxide) 0.03, 0.05, 0.1, 0.3, and 0.5 ppm of IPC in toluene  
47 [21]. The liquid IPC (> 99.99%) used to prepare the volatile standards was purchased from Sigma-  
48 Aldrich.  
49

50 TOF-SIMS (ION-TOF SIMS IV) depth profiling was performed to obtain the depth distribution and  
51 chemical composition of deposited film as a function of IPC concentration in the feed. As the layer  
52 coating the silicon substrate using the new cylinder is not sufficiently thick for reliable analysis (few  
53 nanometers), both TOF-SIMS and XPS analyses were performed on samples produced with the old  
54 cylinder. The TOF-SIMS analysis was carried out without any sample preparation or further pretreatment.  
55 Depth profiling was measured using a 3.0 kV Cs<sup>+</sup> ion source at a sputtering rate of 0.5 nm/min in a 50  
56 μm × 50 μm analysis area, confined within a 500 μm × 500 μm sputter area. The ion dose densities were  
57 5 × 10<sup>12</sup> ions cm<sup>-2</sup>. Negative ion depth profiles of various species were retained for analysis as they have  
58 better sensitivity to oxide fragments.  
59  
60  
61  
62  
63  
64  
65

### 3. Results and Discussion

#### 3.1. Gas Phase

To identify and quantify the IPC in both CO cylinders, the ion-level data was extracted from the total ion chromatograms. The extracted ion chromatograms (EIC) show peaks for five ions with mass over charge ratio ( $m/z$ ) of 56, 84, 112, 140, and 168 at the same retention time of 1.22 min. These correspond to different species derived by the fragmentation of the IPC in the mass spectrometer via ionization; in other words, the fingerprint of IPC. For both the old and new cylinders, Fe ( $m/z = 56$ ) and Fe(CO) ( $m/z = 84$ ) are the most abundant peaks at a retention time of 1.22 min (Fig. 2a and b). Based on the peak areas, in six months, the IPC concentrations increased by an order of magnitude, from  $0.020 \pm 0.005$  ppm to  $0.21 \pm 0.06$  ppm. CO reacts with the iron in the cylinder slowly with time [22, 23]. Given that IPC concentration is the only parameter we found to vary over this six-month period, and that we observed a significant increase in deposition rate (Fig. 2c), we hypothesized that IPC has a determinant role in the photochemical reactions taking place at the solid-gas interphase. In other words, IPC is likely to have initiated or catalyzed the reaction and the reaction rate depends on its concentration in the CO feed.

Fig. 2 (a), (b) Extracted ion chromatograms of gas samples from new and old carbon monoxide cylinders and (c) coated wafers using those cylinders (the narrow black margins on the right-hand side of the coupons show the pristine silicon wafer surface were shielded by Kapton tape during treatment). The insets show the calibration of IPC concentration for five standard samples quantified based on the same ions.

#### 3.2. Solid Phase (film)

Fig.3 (a) and (b) represent inorganic/oxide and organic species abundance as a function of depth within the film, respectively. Organometal and oligomer species were initially higher than silicon, indicating formation of a 38 nm thick film on the substrate. Si signals ( $\text{SiO}_2$ , Si,  $\text{Si}^{2-}$ ,  $\text{Si}^{3-}$ ) then start to increase indicating the complete removal of deposited film and digging into the substrate. Presence of silica along with other species during the layer-by-layer removal shows that the deposited film only partially covered the substrate, in the form of isolated islands [17]. At depths of 40 nm and 45 nm, silicon oxide, silanol groups and silicon appear, indicating a 5 nm layer of Si-OH, which is the main free reaction site on the surface. The Si-C profile confirms the formation of a covalent bond between the oligomeric chains and these silanol sites.

Fig. 3 TOF-SIMS depth profiles of (a) iron species, and (b) oligomer species deposited on the surface of silicon substrate.

Using the silicon species' intensity as a reference (substrate), iron carbonyl fragments appear dominant: namely Fe(CO), Fe(CO)<sub>2</sub> and their derivatives (e.g. FeCOH). This is confirmed by comparing the UVC emission lines to the energy levels determined by Poliakoff and Weitz [8]: UVC has enough energy to dissociate Fe(CO)<sub>5</sub> to its various carbonyl fragments (Fig.4).

These short-lived species must bond with other molecules to form stable compounds. Thus, ligand replacement of CO for other components, e.g. hydrogen and oligomer carbon chains, could occur through a photo-dissociation of Fe(CO)<sub>5</sub>. The TOF-SIMS analysis indicated that Fe(CO) is the dominant species formed – this covalently unsaturated species plays the role of a catalytic initiator in the reaction. This contrasts with previous studies performed under lower energy light sources where, as expected,

1  
2  
3  
4 dissociation could only go to  $\text{Fe}(\text{CO})_2$  and  $\text{Fe}(\text{CO})_3$  [8, 13]. This demonstrates that the reaction depends  
5 on the wavelength of light source.  
6

7 The determinant role played by  $\text{Fe}(\text{CO})_x$  species in photochemical process is evidenced by the presence of  
8 elemental iron and its derivatives (e.g.  $\text{FeC}$  and  $\text{FeH}$ ) (Fig.3a) in the film. Moreover, carbon compounds  
9 in different forms (from C1 to C7, formed in the photoreactor [19]) are attached to at least one iron atom  
10 (Fig.3b). It is pertinent to note that the presence of pure Fe atoms in the film confirms the involvement of  
11 the VUV peak (185 nm) from the mercury lamps (Fig.4) [24].  
12  
13  
14

15  
16 Fig. 4 Energy levels of the UVC lamp at 184.5 and 253.7 nm along with the energy levels required for the formation of  $\text{Fe}(\text{CO})_n$   
17 fragments extracted from Poliakoff and Weitz [8].  
18  
19  
20

#### 21 **4. Conclusion**

22 The unexpected presence of photoreactive IPC in the syngas feed modifies the photo-initiated CVD  
23 polymerization mechanism under UVC light, serving as a homogeneous catalyst. The iron detected in the  
24 oligomer film is traced back to IPC formed in the high-pressure carbon monoxide cylinder, and its effects  
25 are concentration-dependent (which implies time dependency). At atmospheric pressure and ambient  
26 temperature, UVC irradiation of the IPC-containing syngas predominantly forms  $\text{Fe}(\text{CO})$ , which initiates  
27 the reaction. Further experiments are required to understand the kinetics of the surface reaction and the  
28 reaction rate dependency to the IPC concentration and irradiance of UVC lamps. With this knowledge,  
29 control over the IPC concentration in the CO stream will be possible. This case study should serve as  
30 warning to researchers making use of CO cylinders to feed a variety of reactions: IPC may be playing an  
31 unexpected role in your research.  
32  
33  
34

#### 35 **5. Acknowledgements**

36  
37 The authors acknowledge financial support from the Natural Sciences and Engineering Research Council  
38 of Canada (NSERC), the Fonds de recherche du Québec- Nature et Technologies (FRQNT), the Canada  
39 Foundation for Innovation (CFI), Sigma-Xi (G20141015728200), and Hydro-Québec for financial  
40 support of this work. We also thank Dr. J. Lefebvre for TOF-SIMS support.  
41  
42  
43

#### 44 **References**

- 45 [1] G. Friedrich, F.L. Ebenhöch, B. Kühborth, Ullmann's Encyclopedia of Industrial Chemistry, 6th Edition, Electronic  
46 Release, Chapter 3, Wiley-VCH, Weinheim, 2000.  
47 [2] V.G. Syrkin, Preparation of iron powder by the thermal decomposition of iron pentacarbonyl, *Sov. Powder. Metall.*  
48 *Met. Ceram.*, 3 (1965) 232-239.  
49 [3] J. Dewar, H.O. Jones, The physical and chemical properties of iron carbonyl, *Proc. R Soc. Lond. A. Math. Phys.*  
50 *Sci.*, 76 (1905) 558-577.  
51 [4] G. Geoffroy, *Organometallic Photochemistry*, Elsevier Science, 1979.  
52 [5] M. Beller, C. Bolm, *Transition Metals for Organic Synthesis : Building Blocks and Fine Chemicals*, Second Revised  
53 and Enlarged Edition, 2004.  
54 [6] J. Falbe, *New Syntheses with Carbon Monoxide*, Springer-Verlag Berlin Heidelberg, 1980.  
55 [7] M.J. Mirbach, Photochemical Reactions Between Transition Metal Complexes and Gases at High Pressures, High-  
56 Energy Processes in Organometallic Chemistry, ACS Symposium Series, Chapter 9, 333, 1987, pp. 139-154.  
57 [8] M. Poliakoff, E. Weitz, Shedding light on organometallic reactions: the characterization of tetracarbonyliron  
58 ( $\text{Fe}(\text{CO})_4$ ), a prototypical reaction intermediate, *Acc. Chem. Res.*, 20 (1987) 408-414.  
59 [9] C.P. Casey, C.R. Cyr, Iron carbonyl catalyzed isomerization of 3-ethyl-1-pentene. Multiple olefin isomerizations via  
60 a  $\pi$ -allyl metal hydride intermediate, *J. Am. Chem. Soc.*, 95 (1973) 2248-2253.  
61  
62  
63  
64  
65

- 1  
2  
3  
4 [10] W. Tumas, B. Gitlin, A.M. Rosan, J.T. Yardley, Olefin rearrangement resulting from the gas-phase krypton  
5 fluoride laser photolysis of chromium hexacarbonyl, *J. Am. Chem. Soc.*, 104 (1982) 55-59.
- 6 [11] R.L. Whetten, Laser photocatalytic isomerization and hydrogenation of olefins in the gas phase, *J. Chem. Phys.*, 77  
7 (1982) 3769.
- 8 [12] R.L. Whetten, K.J. Fu, E.R. Grant, Pulsed-laser photocatalytic isomerization and hydrogenation of olefins, *J. Am.*  
9 *Chem. Soc.*, 104 (1982) 4270-4272.
- 10 [13] M.A. Schroeder, M.S. Wrighton, Pentacarbonyliron(0) photocatalyzed hydrogenation and isomerization of olefins,  
11 *J. Am. Chem. Soc.*, 98 (1976) 551-558.
- 12 [14] Y. Ishikawa, C.E. Brown, P.A. Hackett, D.M. Rayner, Excimer laser photolysis of Group 6 metal carbonyls in the  
13 gas phase, *J. Phys. Chem.*, 94 (1990) 2404-2413.
- 14 [15] J.T. Yardley, Fragmentation and molecular dynamics in the laser photodissociation of iron pentacarbonyl, *J. Chem.*  
15 *Phys.*, 74 (1981) 370.
- 16 [16] D. Farhanian, C.A. Dorval Dion, W. Raphael, G. De Crescenzo, J.R. Tavares, Combined extraction and  
17 functionalization of low-cost nanoparticles from municipal solid waste fly ash through PICVD, *J. Environ. Chem.*  
18 *Eng.*, 2 (2014) 2242-2251.
- 19 [17] A. Berard, G.S. Patience, G. Chouinard, J.R. Tavares, Photo initiated chemical vapour deposition to increase  
20 polymer hydrophobicity, *Sci. Rep.*, 6 (2016) 31574.
- 21 [18] C.A. Dorval Dion, W. Raphael, E. Tong, J.R. Tavares, Photo-initiated chemical vapor deposition of thin films  
22 using syngas for the functionalization of surfaces at room temperature and near-atmospheric pressure, *Surf. Coat.*  
23 *Technol.*, 244 (2014) 98-108.
- 24 [19] D. Farhanian, G. De Crescenzo, J.R. Tavares, Kinetics, Chemistry, and Morphology of Syngas Photoinitiated Chemical  
25 Vapor Deposition, *Langmuir*, 33(8) (2017) 1780-1791.
- 26 [20] (a) M. Poliakoff, J.J. Turner, A new route to matrix isolated iron atoms, *J. Chem. Soc., Faraday Trans. 2*, 70 (1974)  
27 93. (b) M. Poliakoff, J.J. Turner, Infrared spectrum and photochemistry of di-iron enneacarbonyl in matrices at 20  
28 K: evidence for the formation of  $\text{Fe}_2(\text{CO})_8$ , *J. Chem. Soc. A: Inorganic, Physical, Theoretical*, (1971) 2403. (c)  
29 S.C. Fletcher, M. Poliakoff, J.J. Turner, Structure and reactions of octacarbonyldiiron: An IR spectroscopic study  
30 using carbon-13 monoxide, photolysis with plane-polarized light, and matrix isolation, *Inorg. Chem.*, 25 (1986)  
31 3597-3604. (d) M. Poliakoff, E. Weitz, Shedding light on organometallic reactions: the characterization of  
32 tetracarbonyliron ( $\text{Fe}(\text{CO})_4$ ), a prototypical reaction intermediate, *Acc. Chem. Res.*, 20 (1987) 408-414. (e) S.K.  
33 Nayak, T.J. Burkey, Photosubstitution of iron pentacarbonyl, with triethylphosphine in cyclohexane:  $\text{Fe}(\text{CO})_4\text{PEt}_3$   
34 and  $\text{Fe}(\text{CO})_3(\text{PEt}_3)_2$  are single-photon products, *Inorg. Chem.*, 31 (1992) 1125-1127. (f) J.T. Yardley,  
35 Fragmentation and molecular dynamics in the laser photodissociation of iron pentacarbonyl, *J. Chem. Phys.*, 74  
36 (1981) 370. (g) R.J. Ryther, E. Weitz, Diode laser probes of the product distribution of coordinatively unsaturated  
37 iron carbonyls produced following excimer laser photolysis of iron pentacarbonyl in the gas phase, *J. Phys.*  
38 *Chem.*, 96 (1992) 2561-2567. (h) H.F.D. I. M. Waller, and J. W. Hepburn, Photofragment Spectroscopy of Metal  
39 Carbonyls: A Molecular Beam Study of  $\text{Fe}(\text{CO})_5$ , Photolysis at 193 nm, *J. Phys. Chem.*, 91 (1987) 506-508. (i)  
40 B.K. Venkataraman, G. Bandukwalla, Z. Zhang, M. Vernon, One- and two-photon photodissociation of  $\text{Fe}(\text{CO})_5$   
41 at 248 nm. Application of an accurate method for calculating angle resolved velocity distributions for multiple  
42 sequential bond rupture processes, *J. Chem. Phys.*, 90 (1989) 5510. (j) U. Ray, S.L. Brandow, G. Bandukwalla,  
43 B.K. Venkataraman, Z. Zhang, M. Vernon, A crossed laser-molecular beam study of the photodissociation  
44 dynamics of  $\text{Fe}(\text{CO})_5$  at 193 nm, *J. Chem. Phys.*, 89 (1988) 4092. (k) D.M. Hayes, E. Weitz, A study of the  
45 kinetics of reaction of iron tricarbonyl and  $\text{Fe}(\text{CO})_3(\text{L})$  with hydrogen and ethene for  $\text{L} = \text{hydrogen}$  and ethene by  
46 transient Infrared spectroscopy: reactions relevant to olefin hydrogenation kinetics, *J. Phys. Chem.*, 95 (1991)  
47 2723-2727. (l) H. Morita, Y. Takeyasu, H. Okamura, H. Ishikawa, Magnetic field effect on gas-phase synthesis of  
48 metal-containing ultrafine particles from iron pentacarbonyl and carbon disulfide, *Sci. Tech. Adv. Mater.*, 7 (2006)  
49 389-394. (m) M.A. Henderson, R.D. Ramsier, J.T. Yates, Photochemical activity of iron pentacarbonyl on  
50  $\text{Ag}(111)$ : photofragmentation, quenching and wavelength-dependent effects, *Surf. Sci.*, 275 (1992) 297-313. (n) S.  
51 Sato, Y. Ukisu, Mechanism of the photolysis of iron pentacarbonyl adsorbed on a Pt surface, *Surf. Sci.*, 283  
52 (1993) 137-142. (o) G. Nathanson, Ultraviolet laser photolysis: Primary photochemistry of  $\text{Fe}(\text{CO})_5$  in  $\text{PF}_3$ , *J.*  
53 *Chem. Phys.*, 74 (1981) 361. (p) R.L. Whetten, K.J. Fu, E.R. Grant, Pulsed-laser photocatalytic isomerization and  
54 hydrogenation of olefins, *J. Am. Chem. Soc.*, 104 (1982) 4270-4272. (q) A.J. Ouderkirk, P. Wermer, N.L. Schultz,  
55 E. Weitz, Observation of coordinatively unsaturated intermediates following the pulsed UV photolysis of iron  
56 pentacarbonyl ( $\text{Fe}(\text{CO})_5$ ), *J. Am. Chem. Soc.*, 105 (1983) 3354-3355. (r) A.J. Ouderkirk, E. Weitz, The kinetics of  
57 reaction of photolytically generated  $\text{Fe}(\text{CO})_x$  ( $x=2,3,4$ ) with CO, *J. Chem. Phys.*, 79 (1983) 1089. (s) R.L.  
58 Whetten, Laser photocatalytic isomerization and hydrogenation of olefins in the gas phase, *J. Chem. Phys.*, 77  
59 (1982) 3769. (t) T.A. Seder, A.J. Ouderkirk, E. Weitz, The wavelength dependence of excimer laser photolysis of  
60  $\text{Fe}(\text{CO})_5$  in the gas phase. Transient infrared spectroscopy and kinetics of the  $\text{Fe}(\text{CO})_x$  ( $x=4,3,2$ ) photofragments,  
61 *J. Chem. Phys.*, 85 (1986) 1977. (u) N. Bottka, P.J. Walsh, R.Z. Dalbey, Photolysis of  $\text{Fe}(\text{CO})_5$  adsorbed on GaAs  
62 at 77 K, *J. Appl. Phys.*, 54 (1983) 1104. (v) P.M. George, J.L. Beauchamp, Deposition of metal films by the  
63 controlled decomposition of organometallic compounds on surfaces, *Thin Solid Films*, 67 (1980) L25-L28. (w)  
64 M.v.E. J.B. Nagy, E.G. Derouane, Highly dispersed supported iron particles from the decomposition of iron  
65 carbonyl on HY zeolite, *J. Catal.*, 58 (1979) 230-237. (x) P.J. Krusic, ESR study of paramagnetic iron carbonyl



1  
2  
3  
4 hydrides, *J. Am. Chem. Soc.*, 103 (1981) 2131-2133. (y) J.J. Turner, M.B. Simpson, M. Poliakoff, W.B. Maier,  
5 Synthesis and decay kinetics of tricarbonyldinitrogen (Ni(CO)<sub>3</sub>N<sub>2</sub>) in liquid krypton: approximate  
6 determination of the nickel-dinitrogen (Ni-N<sub>2</sub>) bond dissociation energy, *J. Am. Chem. Soc.*, 105 (1983) 3898-  
7 3904. (z) R.K. Upmács, G.E. Gadd, M. Poliakoff, M.B. Simpson, J.J. Turner, R. Whyman, A.F. Simpson, The  
8 photochemical synthesis of [Cr(CO)<sub>5</sub>(H<sub>2</sub>)] in solution: i.r. evidence for co-ordinated molecular dihydrogen, *J.*  
9 *Chem. Soc., Chem. Commun.*, (1985) 27. (aa) J.K. Hoyano, A.D. McMaster, W.A.G. Graham, Activation of  
10 methane by iridium complexes, *J. Am. Chem. Soc.*, 105 (1983) 7190-7191. (ab) W. Strohmeier, H. Steigerwald,  
11 Photoinduzierte, homogene und selektive Hydrierung von 1,3-Cyclohexadien in Substanz mit IrClCO(PPh<sub>3</sub>)<sub>2</sub> bei  
12 Umsatzzahlen bis 100 000, *J. Organomet. Chem.*, 125 (1977) C37-C39. (ac) M.J. Mirbach, N. Topalsavoglou,  
13 T.N. Phu, M.F. Mirbach, A. Saus, Photochemische Hydroformylierung mit Cobaltkatalysatoren in Methanol,  
14 *Chem. Ber.*, 116 (1983) 1422-1440. (ad) M.J. Mirbach, M.F. Mirbach, A. Saus, N. Topalsavoglou, P. Tuyet Nhu,  
15 Photochemical hydroformylation of olefins with cobalt catalysts. 2. Ionic cobalt carbonyls, *J. Am. Chem. Soc.*,  
16 103 (1981) 7594-7601. (ae) A. Saus, T.N. Phu, M.J. Mirbach, M.F. Mirbach, Photochemical hydroformylation of  
17 olefins with rhodium catalysts at elevated pressure, *J. Mol. Catal.*, 18 (1983) 117-125. (af) E. Weitz, Transient  
18 Infrared Spectroscopy as a Probe of Coordinatively Unsaturated Metal Carbonyls in the Gas Phase, *J. Phys.*  
19 *Chem.*, 98 (1994) 11256-11264. (ag) E.N. Frankel, E.A. Emken, V.L. Davison, Homogeneous Hydrogenation of  
20 Methyl Linolenate Catalyzed by Iron Pentacarbonyl. Formation of Methyl Octadecatrienoate—Iron Tricarbonyl  
21 Complexes I, *J. Org. Chem.*, 30 (1965) 2739-2745. (ah) H. Nagorski, M.J. Mirbach, A radical mechanism for the  
22 photochemical iron pentacarbonyl catalyzed hydrogenation of octenes, *J. Organomet. Chem.*, 291 (1985) 199-204.  
23 (ai) M.A. Schroeder, M.S. Wrighton, Pentacarbonyliron(0) photocatalyzed hydrogenation and isomerization of  
24 olefins, *J. Am. Chem. Soc.*, 98 (1976) 551-558. (aj) K.J. Fu, R.L. Whetten, E.R. Grant, Pulsed-laser-initiated  
25 photocatalysis in the liquid phase, *Ind. Eng. Chem. Prod. Res. Dev.*, 23 (1984) 33-40. (ak) J.R. Wells, E. Weitz, A  
26 time-resolved Fourier transform infrared study of the catalytic hydrogenation of ethene following UV photolysis  
27 of mixtures of iron pentacarbonyl C<sub>2</sub>H<sub>4</sub>, and hydrogen, *J. Phys. Chem.*, 97 (1993) 3084-3087. (al) H. Ihee, J. Cao,  
28 A.H. Zewail, Ultrafast Electron Diffraction of Transient [Fe(CO)<sub>4</sub>]: Determination of Molecular Structure and  
29 Reaction Pathway, *Angew. Chem. Int. Ed.*, 40 (2001) 1532-1536. (am) J.C. Mitchener, M.S. Wrighton, Low-  
30 temperature photochemistry of tetracarbonyl ethyleneiron and tetracarbonyl propyleneiron. Spectroscopic  
31 observation of catalytically significant intermediates, *J. Am. Chem. Soc.*, 105 (1983) 1065-1067. (an) G.T. Long,  
32 E. Weitz, A Study of the Mechanism of Iron Carbonyl-Catalyzed Isomerization of 1-Pentene in the Gas Phase  
33 Using Time-Resolved Infrared Spectroscopy, *J. Am. Chem. Soc.*, 122 (2000) 1431-1442. (ao) G.T. Long, W.  
34 Wang, E. Weitz, A Real Time Spectroscopic Probe of  $\beta$ -Hydrogen Transfer in the Gas Phase: Formation of  
35 HFe(CO)<sub>3</sub>( $\eta$ -3-C<sub>3</sub>H<sub>5</sub>), *J. Am. Chem. Soc.*, 117 (1995) 12810-12818. (ap) H. Fleckner, F.W. Grevels, D. Hess,  
36 Tricarbonylbis( $\eta$ -2-cis-cyclooctene)iron: photochemical synthesis of a versatile tricarbonyliron source for olefin  
37 isomerization and preparative applications, *J. Am. Chem. Soc.*, 106 (1984) 2027-2032. (aq) P.T. Snee, C.K.  
38 Payne, S.D. Mebane, K.T. Kotz, C.B. Harris, Dynamics of Photosubstitution Reactions of Fe(CO)<sub>5</sub>: An Ultrafast  
39 Infrared Study of High Spin Reactivity, *J. Am. Chem. Soc.*, 123 (2001) 6909-6915.

[21] [airgassgcatalog.com](http://airgassgcatalog.com) : carbon monoxide pure gases.

[22] J.G. King, J.A. Sutcliffe, The formation of iron carbonyl on storage of commercial hydrogen under pressure, *J. Soc. Chem. Ind.*, 47 (1928) T-356.

[23] J. Sendroy, H.A. Collison, H.J. Mark, Determination of iron pentacarbonyl in commercial carbon monoxide, *Anal. Chem.*, 27 (1955) 1641-1645.

[24] Persistent Lines of Neutral Mercury (Hg I). [Physics.nist.gov](http://physics.nist.gov), 2016, (accessed 23.12.16).

43  
44  
45  
46  
47  
48  
49  
50  
51  
52  
53  
54  
55  
56  
57  
58  
59  
60  
61  
62  
63  
64  
65

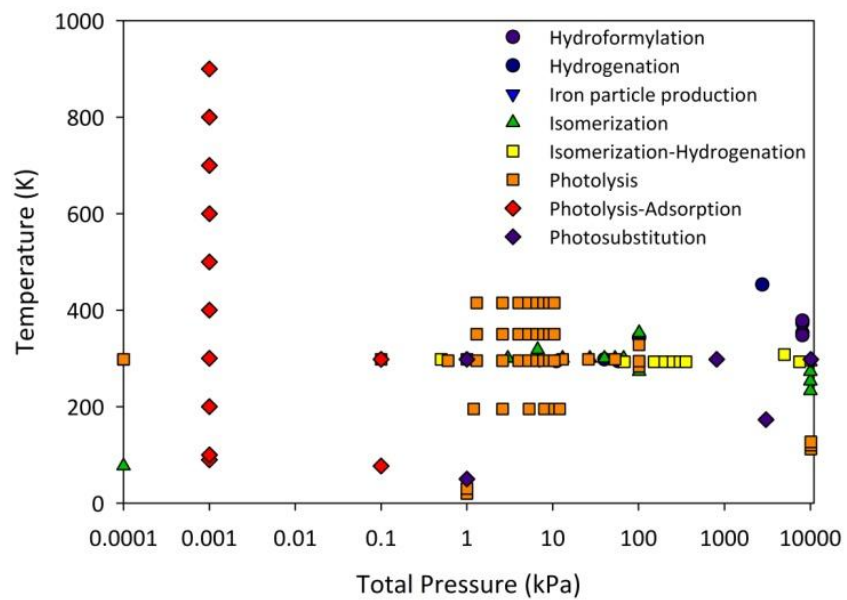


Fig. 1 Operating conditions of previous photolytic IPC reactions [19]

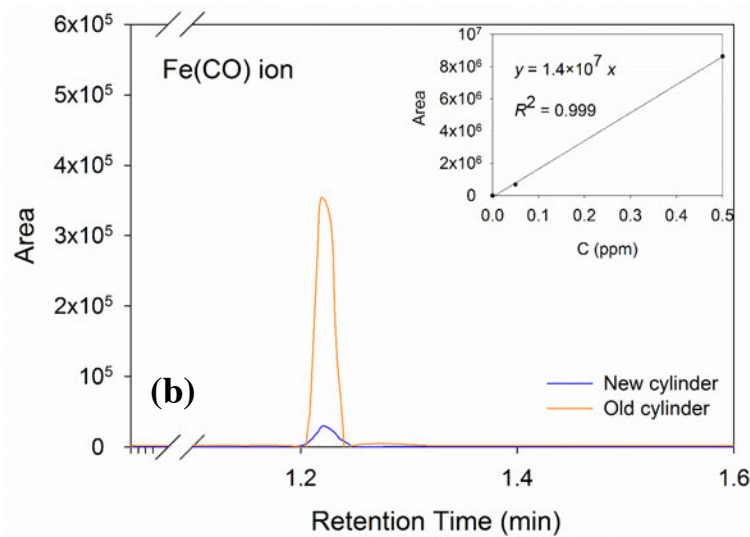
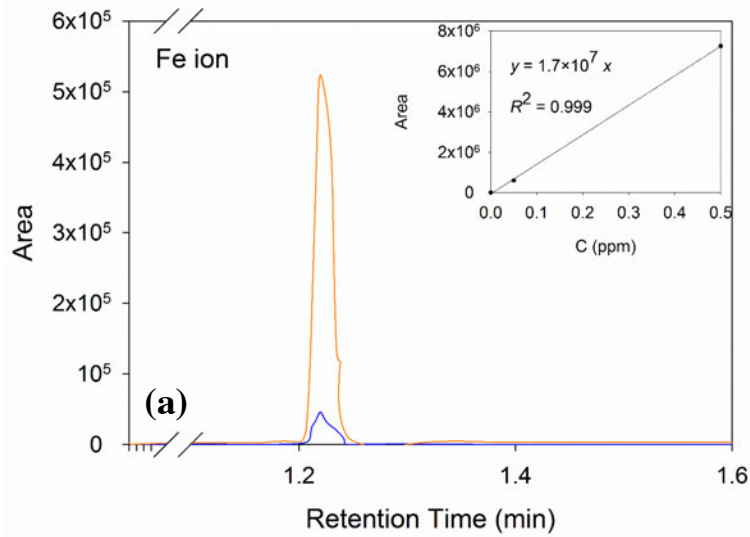


Fig. 2 (a), (b) Extracted ion chromatograms of gas samples from new and old carbon monoxide cylinders and (c) coated wafers using those cylinders (the narrow black margins on the right-hand side of the coupons show the pristine silicon wafer surface were shielded by Kapton tape during treatment). The insets show the calibration of IPC concentration for five standard samples quantified based on the same ions.

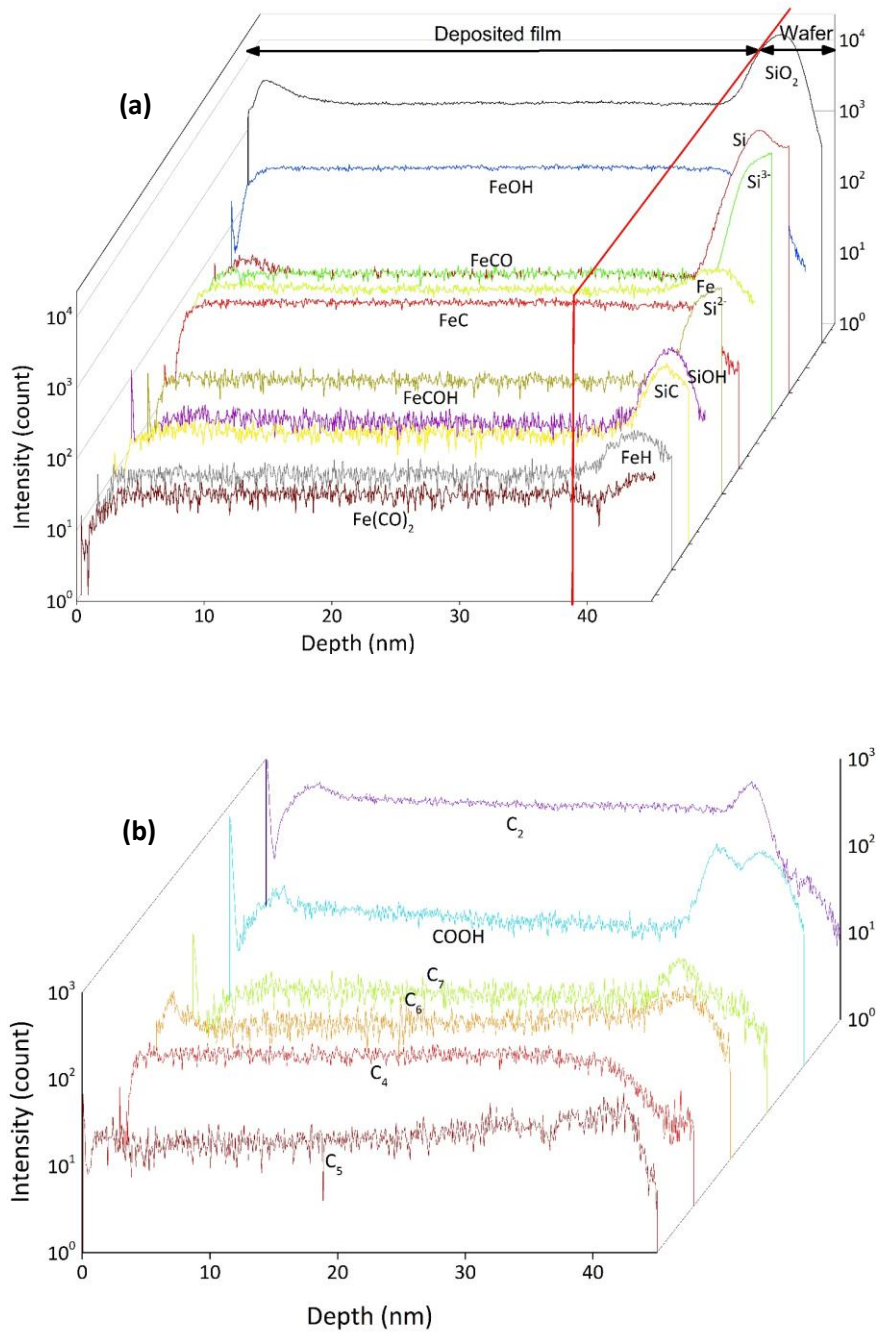


Fig. 3 TOF-SIMS depth profiles of (a) iron species, and (b) oligomer species deposited on the surface of silicon substrate.

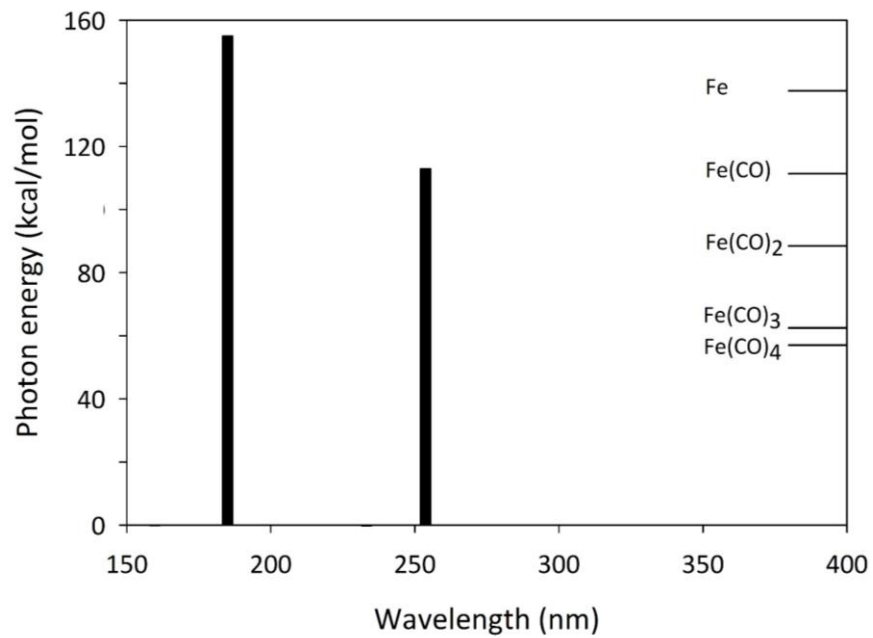


Fig. 4 Energy levels of the UVC lamp at 185 and 253.7 nm along with the energy levels required for the formation of Fe(CO)<sub>n</sub> fragments extracted from Poliakoff and Weitz [8].



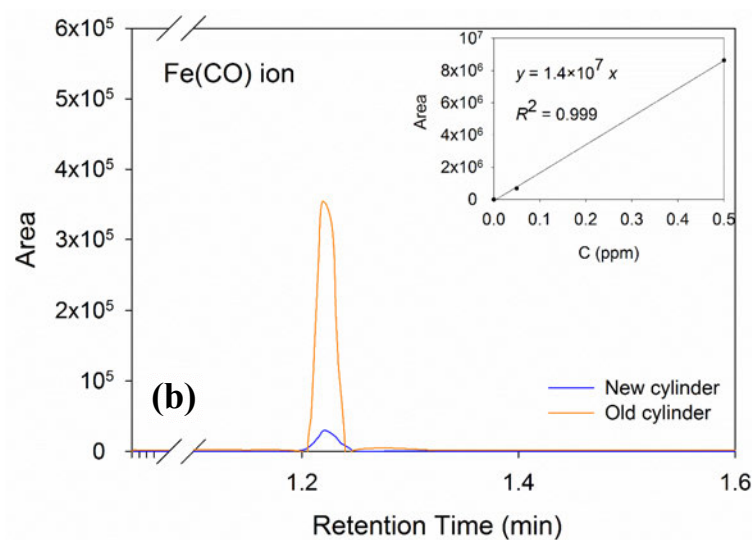
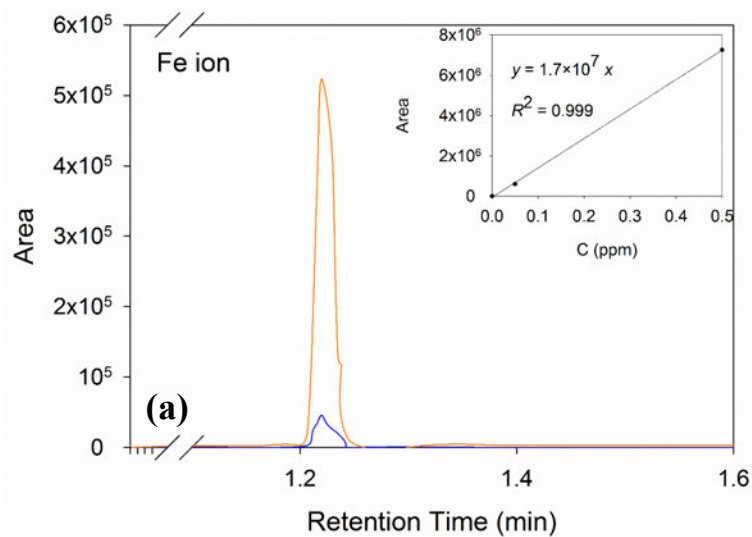


Fig. 2 (a), (b) Extracted ion chromatograms of gas samples from new and old carbon monoxide cylinders and (c) coated wafers using those cylinders (the narrow black margins on the right-hand side of the coupons show the pristine silicon wafer surface were shielded by Kapton tape during treatment). The insets show the calibration of IPC concentration for five standard samples quantified based on the same ions.

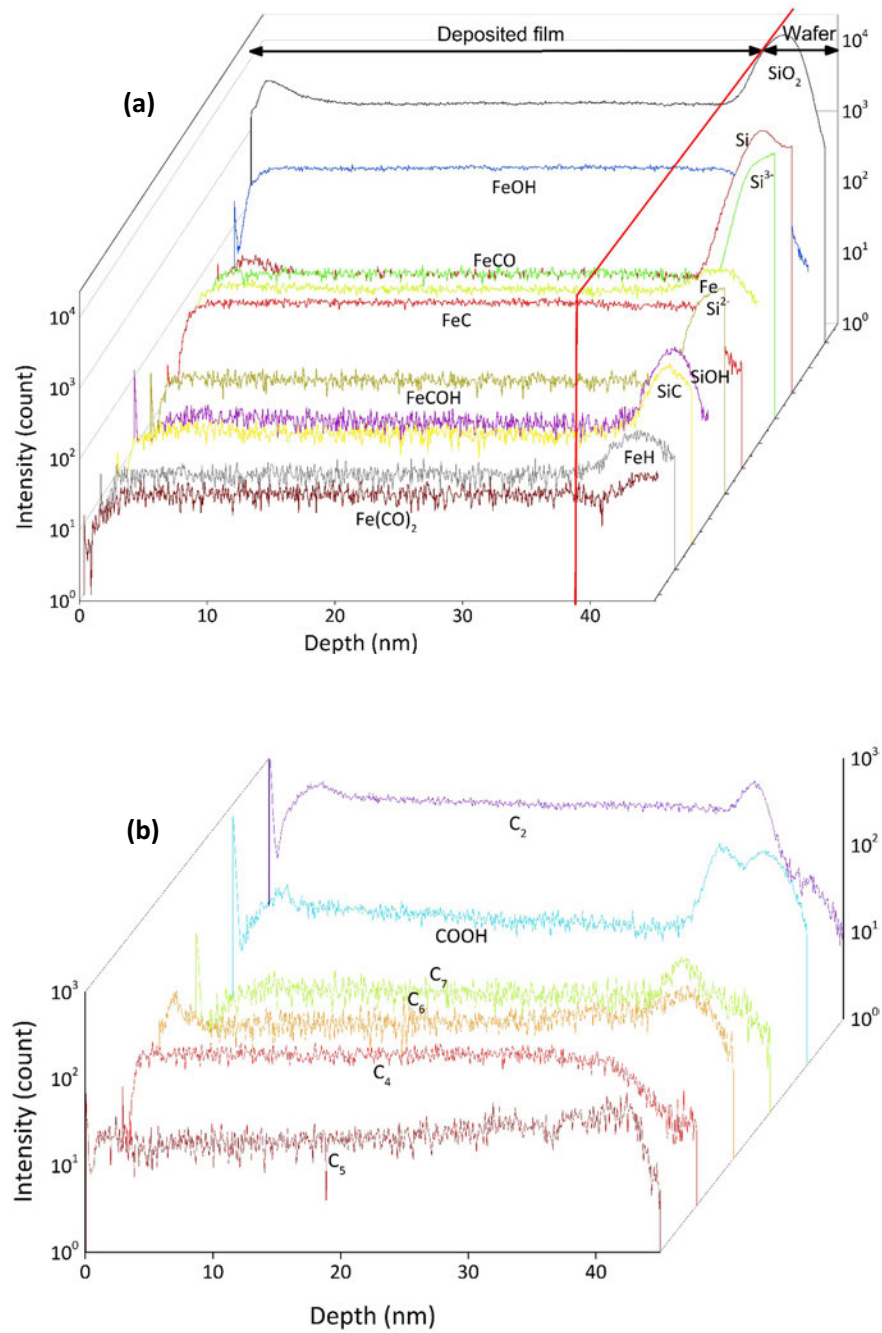


Fig. 3 TOF-SIMS depth profiles of (a) iron species, and (b) oligomer species deposited on the surface of silicon substrate.



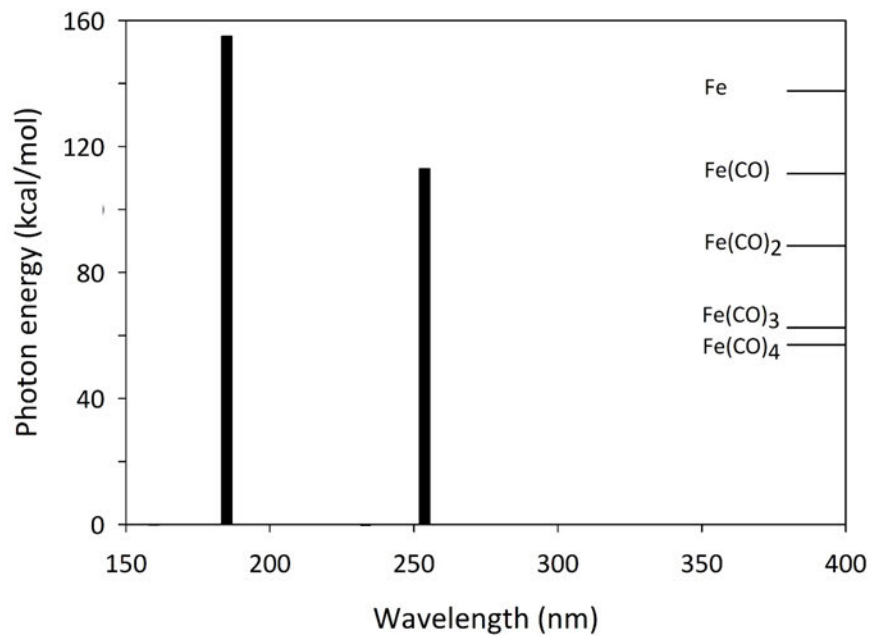


Fig. 4 Energy levels of the UVC lamp at 185 and 253.7 nm along with the energy levels required for the formation of  $\text{Fe}(\text{CO})_n$  fragments extracted from Poliakoff and Weitz [8].

**Supplementary material for online publication only**

**[Click here to download Supplementary material for online publication only: Supporting Information.docx](#)**